Quantitative extraction of spectral line intensities and widths from x-ray spectra recorded with gated microchannel plate detectors

Greg Dunham
Ktech Corporation, 1300 Eubank Boulevard, SE Albuquerque, New Mexico 87123

J. E. Bailey, G. A. Rochau, and P. W. Lake
Sandia National Laboratories, P.O. Box 5800, Albuquerque, New Mexico 87185-1196

L. B. Nielsen-Weber
Ktech Corporation, 1300 Eubank Boulevard, SE Albuquerque, New Mexico 87123

(Received 5 February 2007; accepted 21 May 2007; published online 27 June 2007)

Plasma spectroscopy requires determination of spectral line intensities and widths. At Sandia National Laboratories Z facility we use elliptical crystal spectrometers equipped with gated microchannel plate detectors to record time and space resolved spectra. We collect a large volume of data typically consisting of five to six snapshots in time and five to ten spectral lines with 30 spatial elements per frame, totaling to more than 900 measurements per experiment. This large volume of data requires efficiency in processing. We have addressed this challenge by using a line fitting routine to automatically fit each spectrum using assumed line profiles and taking into account photoelectron statistics to efficiently extract line intensities and widths with uncertainties. We verified that the random data noise obeys Poisson statistics. Rescale factors for converting film exposure to effective counts required for understanding the photoelectron statistics are presented. An example of the application of these results to the analysis of spectra recorded in Z experiments is presented. © *2007 American Institute of Physics.* [DOI: 10.1063/1.2748674]

I. INTRODUCTION

X-ray emission spectroscopy is a powerful diagnostic technique for numerous high energy density (HED) plasmas.[1–5] Applications include laser produced plasmas, *z*-pinch radiation sources, and inertial confinement fusion (ICF) capsule implosions. Information about the plasma electron temperature is commonly obtained by measuring spectral line intensity ratios, while the electron density is inferred from the spectral line shapes. These measurements involve several steps: (1) data acquisition; (2) quantitative extraction of desired line intensities and widths; (3) applying instrument calibrations to the measured intensities and widths; and (4) inference of plasma conditions using an appropriate plasma spectroscopy model.

Each of these steps is complex and must be carefully tailored to the particular experiment. In the first step it is frequently desirable to resolve the temporal and spatial gradients. Hence spectra are often recorded with time-gated microchannel plate (MCP) detectors,[6,7] since this permits the acquisition of a sequence of snapshots that resolve the spectral wavelengths and simultaneously provide one dimensional spatial resolution. The second step is the topic of this paper. The measured spectral lines are fitted with model spectral line profiles, accounting as rigorously as possible for the statistical data fluctuations (noise). The product of this step is a collection of spectral intensities and widths along with their attendant uncertainties. The third step consists of applying instrument calibrations to the measurements in order to determine the properties of the plasma source emission from the signals measured at the detector. It is critical that this step be performed after the fitting performed in step 2, since otherwise the intensity dependence of the statistical fluctuations will be altered and incorrect uncertainties will result. The fourth step includes decisions about the model to be used, approximations appropriate to the application, and which measured intensities and widths offer the greatest sensitivity to the relevant plasma parameters.

The quality of the fit obtained in step 2 is described using the normalized χ^2, defined as

$$\chi^2 = \frac{1}{N-m}\sum_{i=1}\left\{\frac{1}{\sigma_i^2}[y_i - y(x_i)]^2\right\}, \tag{1}$$

where $N-m$ is the number of degreees of freedom for fitting N data points with m parameters, y_i is the data, $y(x_i)$ is the fit, and σ_i^2 is the variance.[8]

The signal in adjacent detector channels must be uncorrelated in order for Eq. (1) to be valid. For MCP detectors the minimum channel size is determined by the 30–50 μm diameter intensity spot that corresponds to the bundle of photoelectrons emerging from the rear of a single MCP channel. The channel size used in the work reported here was 66 $\times$ 66 mm^2 or larger, ensuring that the data statistics are not affected by adjacent channel correlations. In addition, a prescription must be available for the uncertainty (σ_i) of the signal intensity measured in each detector channel. It is commonly assumed that the data obey Poisson statistics and the uncertainty in each channel is equal to the square root of the intensity. The measurements in this article were designed to test whether that assumption is valid for the MCP detectors used in our research.[6]

The Poisson statistics assumption was previously validated for streak camera and x-ray film detectors.[9,10] The strategy followed here was similar. Data are recorded by exposing the detector to a source that illuminates the detector with an intensity that is spatially uniform. If Poisson statistics are a reasonable approximation for the actual detector response, then the fluctuations in the intensity about the mean value will be well represented by a fit with a Poisson distribution. A second test is performed by recording data with a constant intensity source and varying exposure duration to produce a collection of exposures with varying mean signal strengths. The data are converted from film exposure units into counts in each channel using a process described below. If Poisson statistics are valid, then a log plot of the signal-to-noise ratio ($SN=y_i/\sigma_i=y_i^{1/2}$) as a function of signal should be a straight line of slope of 1/2.

The data obtained in these experiments confirm that Poisson statistics are a good approximation for the actual fluctuations in spectra recorded with our MCP detectors. In addition, data were recorded using MCP bias voltages of 500, 600, and 700 V. This enables a determination of whether the mechanism that dominates the noise is the initial conversion of incident x-ray photons into photoelectrons or if the amplification within the MCP pores adds additional noise. We find that most of the noise appears to originate in the initial photoelectron production.

The methods described here also provide techniques for converting experimental spectra from exposure units into counts. This is an essential part of any fitting method that seeks to quantitatively determine the uncertainties in spectral line intensities and widths. An illustration of the extraction of quantitative information from ICF capsule implosions conducted at the Sandia National Laboratories Z facility is described in Sec. IV.

II. EXPERIMENT

The experimental setup was similar to Fig. 1 of Ref. 9. A Manson source using a silver anode was used to uniformly expose a six strip MCP to x rays. The spectrum from this source consists primarily of characteristic Ag L lines.[11] The distance between the x-ray source and detector was approximately 2 m. A 12.7 μm beryllium filter was placed in front of the MCP detector to block visible light. The MCP detector was the type used in recent Z experiments[2–5,12] with sensitivity calibrations described in Ref. 6. Each strip line was 40 mm across and 4 mm tall, with a 0.75 mm gap between each strip line. The MCP used was manufactured by Burle Inc., had a pore length/diameter ratio (L/D) of 46, and had an open area that was 65% of the total surface area. The MCP front surface was coated in four separate layers with the following materials and thicknesses: 75 Å of chromium, 5000 Å of copper, 75 Å of chromium, and 1000 Å of gold. The phosphor type was P43, the phosphor to MCP gap was 0.7 mm, and the phosphor bias was 3000 V. Kodak TMAX 400 film was used to record the signal exiting the MCP detector. Eight to ten exposure times ranging from 30 s to 2 h were chosen so that the full range of optical densities from film fog to near saturation were obtained. MCP bias voltages of 500, 600, and 700 V were used.

The film was developed using a Wing-Lynch Model 5 automatic film processor using the following processing times: water presoak—1 min; T-Max developer—15 min; stop—1 min; fixer—10 min; wash—6 min. The film was scanned on a Perkin-Elmer microdensitometer using matched NA=0.1 optics and a scan box of 22×22 μm^2. MCP detectors have typical spatial resolution of approximately 50 μm, resulting from the lateral spread in electrons as they are accelerated from the MCP rear surface to the phosphor. Therefore, statistically meaningful fits require that the digitization of the MCP data be performed with channel size of approximately 50 μm or greater. In our work we typically digitize the data with a 22×22 μm^2 scanning aperture, then rebin the data by a factor of 3. This process is designed to avoid errors that result when low intensity film data are scanned with an aperture that is larger than the MCP spatial resolution element (see Ref. 10). For each batch of film a calibrated step wedge was exposed and then developed and scanned with the film to minimize any errors caused by variations in development or light intensity during the development and scanning processes. The step wedge was processed to generate a density versus exposure correction curve which was then applied to all of the image data from a single batch to convert it from optical density to film exposure.

III. DATA ANALYSIS AND RESULTS

The first approach is to examine whether the MCP fluctuations are well fitted by a Poisson distribution. In that case the uncertainty in the data is equal to the square root of the number of counts.[8]

To construct a probability distribution from the data, lineouts were taken across the length of the strip line. The lineout averages over a 100 μm tall region in the data, the same height used in many capsule implosion experiments.[2] The lineout height is important since the average flux is independent of the height, but the number of counts contributing to the average increases linearly with the height. Thus, the signal-to-noise ratio improves for taller lineouts (see below). Each point in a lineout may be considered an independent measurement of the flux hitting the detector. The distribution of flux values in individual channels about the mean exposure is illustrated in Fig. 1. Figure 1(a) shows a sample image from one exposure time with the black box indicating where the Fig. 1(b) lineout was taken. In Fig. 1(c) a subset of the data points from the lineout are shown with the mean and standard deviation of the distribution marked by the solid and dashed lines, respectively. For each lineout the data are first rebinned by a factor of 3 to ensure that each channel is uncorrelated with its neighbors. The strip line flux measurements are not perfectly spatially uniform, as illustrated in Fig. 1(b). Flux variations over broad spatial scales result from source and detector nonuniformities. In order to account for these broad spatial scale nonuniformities the data are fitted with a second order polynomial, which is subtracted from the data, then the mean is added back in to

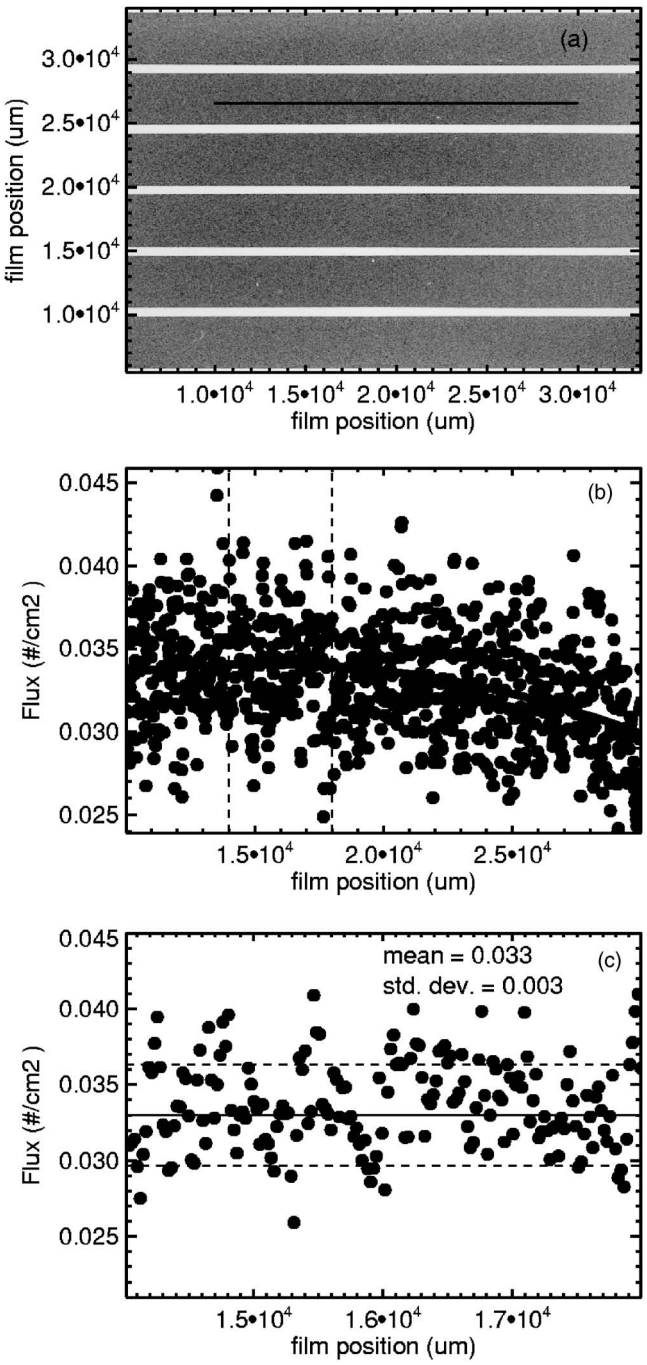

FIG. 1. (a) Sample MCP image with lineout area shown by black line. (b) Points—data from a 100 μm wide lineout taken from the area shown in (a). Black line—second order fit to data. (c) Points—individual flux values to a short 100 μm lineout taken from the region between the dashed lines in part (b). Solid line—mean flux value. Dashed lines—1σ error bars.

retain the original mean flux. The distribution of flux values represented by points were binned into a histogram using 50 uniformly spaced bins spanning the range of flux values to create a plot of frequency of occurrence as a function of flux. The frequency of occurrence for the ith histogram bin is defined as the number of measurements falling within the boundary of that bin. A fit to the histogram is performed using either a Poisson or a Gaussian distribution. Prior to the fit, the data are converted from the original film exposure flux units of ergs/cm^2 into counts, using the rescale factor defined by RSF$=I/E$, where I is the flux expressed in units of counts and E is the flux in units of ergs/cm^2. For data expressed in counts, the Poisson distribution is

$$P(x) = \frac{\mu^x e^{-x}}{x!},$$

where x is the number of recorded counts in a given measurement and $\langle x \rangle$ is the average number of counts recorded over all measurements. For large numbers of counts simplifications lead to the Gaussian distribution, which is

$$P(x) = \frac{1}{\sqrt{2\pi\bar{x}}} \exp\left[-\frac{(x-\bar{x})^2}{2\bar{x}} \right].$$

For Poisson statistics, the standard deviation $\sigma=\sqrt{\mu}$, where μ is the mean. The full width at half maximum for a Gaussian is $\Gamma_{\text{Gauss}}=2.354\sigma$. Thus, there is a well-defined relationship between μ and Γ. Note that *a priori* the correct value of RSF is unknown. However, the correct relationship between the distribution width and the mean will only exist if the correct value of RSF is used. We perform a sequence of fits for each lineout using a range of RSF values. A good quality fit (as determined by the fit χ^2) can only be obtained if the correct value of RSF was used and if the data obey Poisson statistics. The minimum of the fit χ^2 as a function of RSF determines the optimum value of the RSF and the data are judged to obey Poisson statistics if the minimum χ^2 approaches one.

Figure 2 shows sample histograms with fits overlaid for low, medium, and high numbers of counts. The minimum χ^2 value of the fits is shown on each plot. The average chi-squared values for these fits was 1.06 ± 0.2. The quality of the fits confirms that the data fluctuations obey Poisson statistics.

An alternate method of determining whether the data obey Poisson statistics exploits the fact that if Poisson statistics are valid, then a log plot of the signal-to-noise ratio (SN$=I/\sigma_I=I^{1/2}$) as a function of signal I should be a straight line of slope of 1/2. To implement this method, a sequence of eight to ten measurements at varying exposure levels were made. Each measurement provides data recorded on six MCP strip lines. From each strip line a set of 100 lineouts were taken, each 4000 μm long by 100 μm wide, to make a grid of lineouts 5 columns wide and 20 rows high. Individual lineouts were taken over 1/10 the total strip line length in order to minimize contributions to the fluctuations that result from broad scale nonuniformities. This was devised as an alternative to the polynomial fitting method described above. We obtain six collections of 100 lineouts from each exposure measurement, for a total of 600 lineouts. The data from the lineouts are rebinned by a factor of 3. In order to evaluate whether the fluctuations in the data scale according to Poisson statistics, we must convert the exposure E into counts I. This could, in principle, be done using the fitting approach described above, but the volume of data makes this impractical. Instead, we determine the RSF from each lineout by measuring the mean exposure $\langle E \rangle$ and the standard deviation in the exposure σ_E. Then, if we assume that the data obey Poisson statistics, $\sigma_I^2=\langle I \rangle=\text{RSF}*E$. From the definition of the standard deviation we also have $\sigma_I^2=\text{RSF}^2\sigma_E^2$ and therefore RSF$=\langle E \rangle/\sigma_E^2$. We can test the assumption of Poisson

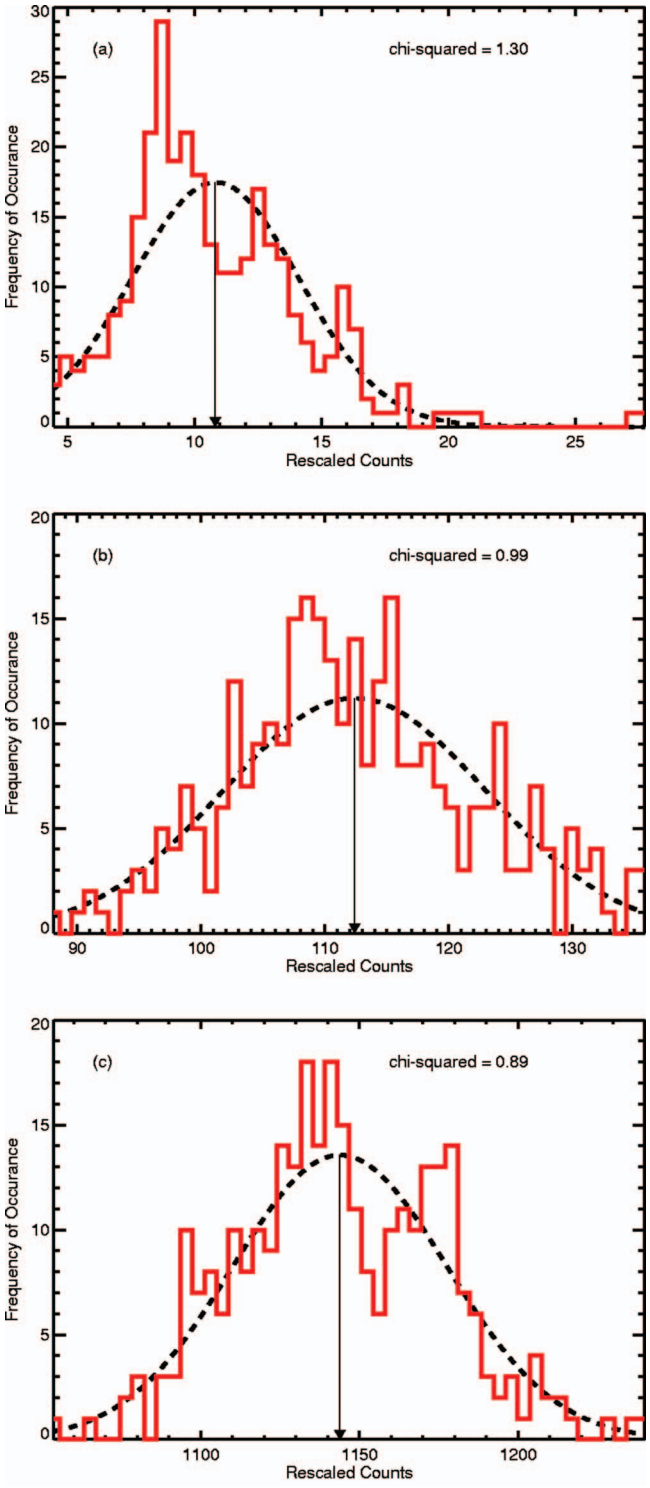

FIG. 2. (Color) Data in red, fit in black dash. Black arrow indicates mean. (a) Low number of counts with a Poisson fit. (b) Medium number of counts with a Gaussian fit. (c). High number of counts with a Gaussian fit.

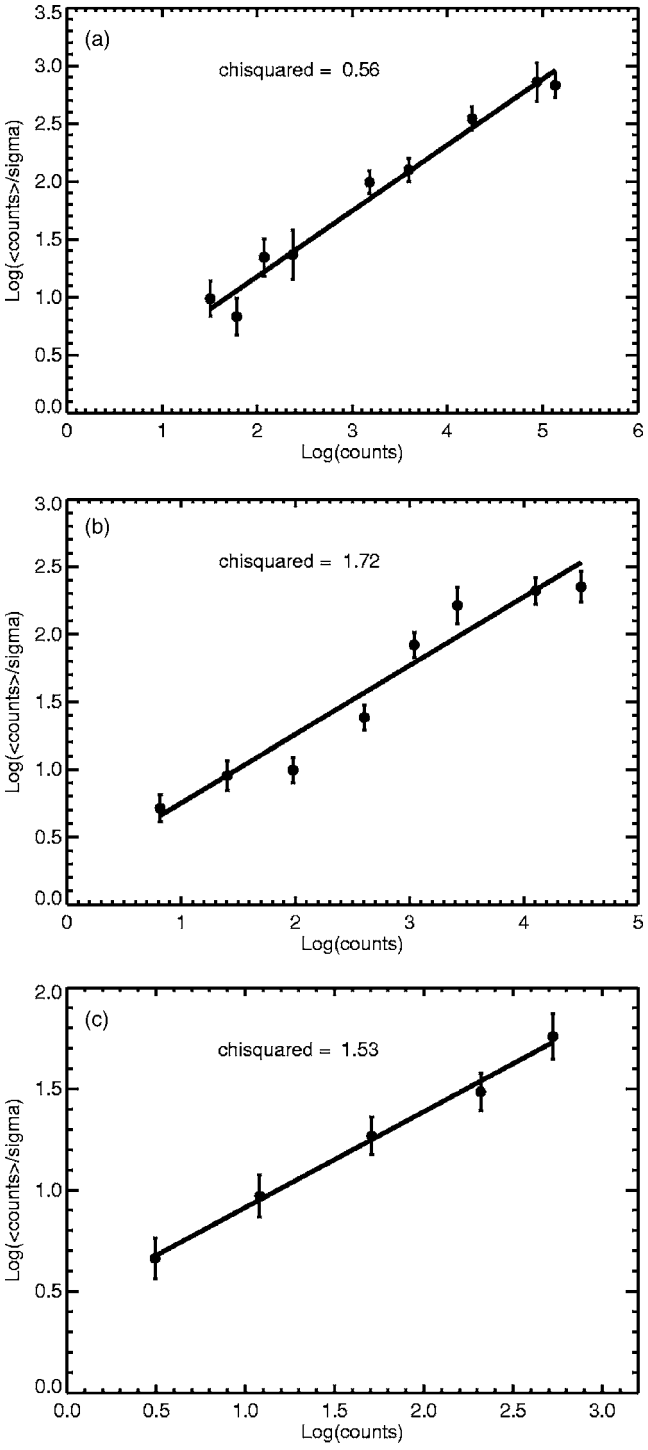

FIG. 3. Data points are average values from 600 measurements at each exposure. Black line is fit to the data. Slopes of the fit lines are 0.57±0.12, 0.51±0.17, and 0.48±0.03, for the 500, 600, and 700 V MCP bias voltages, images (a), (b), and (c), respectively.

statistics by determining the RSF individually from a sequence of measurements at different exposure values and averaging the result. The mean exposure $\langle E \rangle$ from each measurement is converted into counts using the average RSF. We can then construct a log plot of $\mathrm{SN}=I/\sigma_I$ as a function of I. If a linear fit to the collection of data from the different exposures has χ^2 close to 1 and a slope of 1/2, the assumption of Poisson statistics is valid. This process was repeated for the three bias voltages used in the experiment. The slope of the lines fitted to the data were 0.57±0.12, 0.51±0.17, and 0.48±0.03 for the 500, 600, and 700 V bias voltages, respectively (Fig. 3). These results provide an additional confirmation that the MCP detector fluctuations are well represented by Poisson statistics.

The lineout height is selected during the analysis of any HED experiment depending on a balance between competing

TABLE I. MCP voltage vs lineout width scaling data.

MCP voltage	1000 μm/100 μm	400 μm/100μm
700 V	7.201±0.282	3.123±0.183
600 V	8.247±0.684	3.658±0.301
500 V	6.724±1.726	3.256±0.365
Average	7.34±0.26	3.27±0.14

desires for good spatial resolution and signal to noise. The rescale factor RSF should be linearly dependent on the lineout height, as described above. To evaluate this dependence, the above analysis was repeated using 400 and 1000 μm tall lineouts. The resulting RSF values are shown in Table I, in comparison with the original 100 μm tall lineout result. The RSF values increase with lineout height, but the increase is 73%–82% of the linear dependence that is expected. This discrepancy is not fully understood but may be due to systematic nonrandom fluctuations in the data that grow in importance as the lineout area increases.

The confirmation that Poisson statistics are a valid approximation for MCP data analysis does not rely on understanding the exact origin of data fluctuations. Nevertheless, it is an interesting question whether the bulk of the statistical fluctuations arise in the initial conversion of x-ray photons into photoelectrons or if additional noise is added during the acceleration of the photoelectron cascade through the MCP pores that provide the gain. The answer to this question helps determine the optimum gain setting for a particular experiment. In order to begin answering this question we can examine whether $\mathrm{SN}=\sqrt{\mathrm{RSF}*E}$ is independent of the MCP gain that is controlled by the applied bias voltage. If so, then the noise must originate in the initial conversion process (Fig. 4). Each group of points represents the average signal to noise compiled from 600 measurements at a given exposure time. Data for five exposure times of 1, 2, 4, 8, and 16 min are shown. There is a significant amount of scatter in these data but the data are consistent with the claim that no significant degradation in SN occurs as the bias voltage is increased. This result is similar to the findings in Ref. 10 and implies that the SN is dominated by the initial photoelectrons

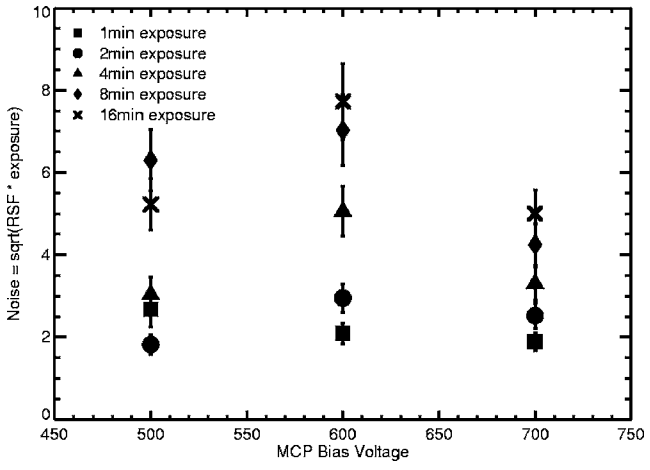

FIG. 4. Average signal to noise for a given exposure time at the three bias voltages of 500, 600, and 700 V.

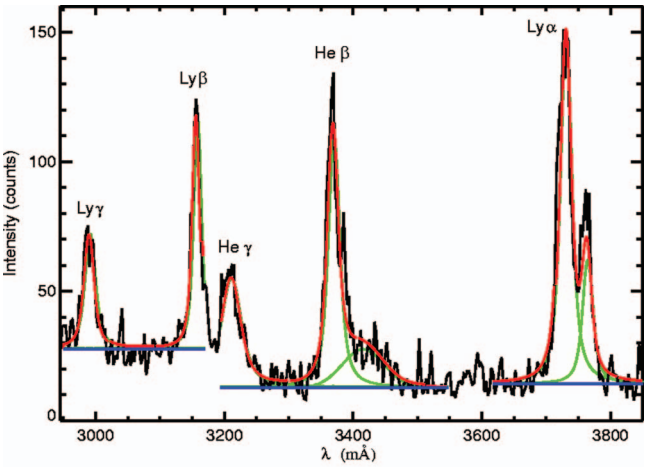

FIG. 5. (Color) Fit to spectra from ICF capsule experiment. Black line—data. Blue line—base line. Green line—fit to individual lines. Red line—composite fit to spectrum.

produced at the MCP pore entrance, prior to any gain. More definitive information would require additional experiments.

IV. DISCUSSION

The results and methods developed here are illustrated by application to x-ray spectra from an ICF capsule implosion experiment described in Ref. 2. A sequence of space-resolved 50 μm tall lineouts were taken on the data shown in Fig. 8 of Ref. 2, at the time snapshot designated $t=-0.1$ ns. The 50 μm lineout height corresponds to the size at the source plasma and is equal to 100 μm at the detector, the same size as in the calibrations described above. In order to fit the lineouts we must first determine the RSF that converts the data from flux in erg/cm^2 into counts. Ideally, this could be done using calibrations that uniformly expose the detector to x rays, with the detector operated in the same pulsed mode that is employed in the HED experiment. In practice, resource limitations prevent such calibrations. Instead, we determine the RSF using the methods described above to analyze the fluctuations in a portion of the lineout that consists of continuum with no spectral lines. In this experiment we used the bound-free recombination between approximately 3.03–3.12 Å. This has limited accuracy since the number of channels is small compared to the number used in the calibrations described here. We overcome this problem by averaging the RSF determined from multiple MCP frames and from as many multiple HED experiments as possible, subject to the constraints that every MCP detector must be analyzed separately and that changes between experiment series make it impractical to compare measurements that are not from the same experimental campaign. In this case measurements from seven frames were averaged to yield a rescale factor of 1084±103.

After converting the spectrum to counts we fit the lineouts using the line fitting code ROBFIT.[13] An example for high-intensity data near the center of the spatial distribution is shown in Fig. 5. ROBFIT determines the intensity, width, and wavelength for each spectral feature self-consistently with the underlying continuum. Various line shape standards

are available, although for these data reasonable fits were obtained using Voigt standards with a Voigt parameter equal to 1. The continuum intensity is different in different wavelength regions because of the wavelength dependence of the free-free and free-bound contributions. We therefore divide the spectrum into three regions and use a constant continuum in each region. The data are shown in black and the composite fit is shown in red. The blue lines indicate the base line determined for each fit region and the green lines are the fits to the individual peaks. The overall χ^2 of the fits ranges from 0.6 to 1.1, indicating that the fits are a reasonable representation of the data and that the uncertainties in the data are consistent with the intensity. The uncertainties in unblended line intensities are typically $\pm 4\% - 8\%$. Blended lines (such as $He\beta$ or $Ly\alpha$ and their satellites) often have somewhat larger uncertainties. Systematic errors that might result from the fitting process are not included in these values. For example, if the actual line profile deviates from the standard profile that was selected, a systematic error would result. Our analysis tabulates the local χ^2 in the vicinity of each line, in addition to the overall χ^2. This enables the detection of possible systematic errors. In the Fig. 5 data the $He\beta$ profile is slightly asymmetric and the local $\chi^2 \sim 2.7$, indicating that additional physics may need to be considered in order to extract the maximum amount of information from this line.

ACKNOWLEDGMENTS

This work was performed at Sandia National Laboratories. Sandia is a multiprogram laboratory operated by Sandia Corporation, a Lockheed Martin Company, for the United States Department of Energy under Contract No. DE-AC04-94-AL85000.

[1] H. R. Griem, *Principles of Plasma Spectroscopy* (Cambridge University Press, 1997).
[2] J. E. Bailey *et al.*, Phys. Plasmas **13**, 056301 (2006).
[3] J. E. Bailey *et al.*, Phys. Rev. Lett. **92**, 085002 (2004).
[4] G. A. Rochau, J. E. Bailey, and J. J. MacFarlane, Phys. Rev. E **72**, 066405 (2005).
[5] S. A. Slutz *et al.*, Phys. Plasmas **10**, 1875 (2003).
[6] G. A. Rochau *et al.*, Rev. Sci. Instrum. **77**, 10E323 (2006).
[7] J. D. Kilkenny, Laser Part. Beams **9**, 49 (1991).
[8] P. R. Bevington and D. K. Robinson, *Data Reduction and Error Analysis for the Physical Sciences* (McGraw-Hill, New York, 1992).
[9] G. Dunham, G. A. Rochau, P. W. Lake, L. Nielsen-Weber, and D. Schuster, Rev. Sci. Instrum. **75**, 3687 (2004).
[10] J. E. Bailey, R. Adams, A. L. Carlson, C. H. Ching, and A. B. FilukRev. Sci. Instrum. **68**, 1099 (1997).
[11] P. W. Lake, J. E. Bailey, G. A. Rochau, D. Petmecky, and P. GardRev. Sci. Instrum. **75**, 3960 (2004).
[12] P. W. Lake *et al.*, Rev. Sci. Instrum. **77**, 10F315 (2006).
[13] R. L. Coldwell and G. J. Bamford, *The Theory and Operation of Spectral Analysis Using ROBFIT* (American Institute of Physics, Melville, New York, 1991).